Biochemical and Biophysical Research Communications 445 (2014) 445–450

Contents lists available at ScienceDirect

Biochemical and Biophysical Research Communications

journal homepage: www.elsevier.com/locate/ybbrc

A surface plasmon resonance study of the intermolecular interaction between *Escherichia coli* topoisomerase I and pBAD/Thio supercoiled plasmid DNA

Purushottam Babu Tiwari [a], Thirunavukkarasu Annamalai [b], Bokun Cheng [c], Gagandeep Narula [b], Xuewen Wang [a], Yuk-Ching Tse-Dinh [b,*], Jin He [a,*], Yesim Darici [a,*]

[a] Department of Physics, Florida International University, Miami, FL 33199, United States
[b] Department of Chemistry and Biochemistry, Florida International University, Miami, FL 33199, United States
[c] Department of Biochemistry and Molecular Biology, New York Medical College, Valhalla, NY 10595, United States

ARTICLE INFO

Article history:
Received 28 January 2014
Available online 12 February 2014

Keywords:
Surface plasmon resonance
Bacterial topoisomerase I
Supercoiled plasmid DNA
Capture covalent method
Equilibrium dissociation constant

ABSTRACT

To date, the bacterial DNA topoisomerases are one of the major target biomolecules for the discovery of new antibacterial drugs. DNA topoisomerase regulates the topological state of DNA, which is very important for replication, transcription and recombination. The relaxation of negatively supercoiled DNA is catalyzed by bacterial DNA topoisomerase I (topoI) and this reaction requires Mg^{2+}. In this report, we first quantitatively studied the intermolecular interactions between *Escherichia coli* topoisomerase I (EctopoI) and pBAD/Thio supercoiled plasmid DNA using surface plasmon resonance (SPR) technique. The equilibrium dissociation constant (K_d) for EctopoI–pBAD/Thio interactions was determined to be about 8 nM. We then studied the effect of Mg^{2+} on the catalysis of EctopoI–pBAD/Thio reaction. A slightly higher equilibrium dissociation constant (~15 nM) was obtained for Mg^{2+} coordinated EctopoI (Mg^{2+}EctopoI)–pBAD/Thio interactions. In addition, we observed a larger dissociation rate constant (k_d) for Mg^{2+}EctopoI–pBAD/Thio interactions (~0.043 s^{-1}), compared to EctopoI–pBAD/Thio interactions (~0.017 s^{-1}). These results suggest that enzyme turnover during plasmid DNA relaxation is enhanced due to the presence of Mg^{2+} and furthers the understanding of importance of the Mg^{2+} ion for bacterial topoisomerase I catalytic activity.

1. Introduction

The drug resistance of bacterial pathogens to available antibacterial drugs is a serious public health issue and needs to be addressed. The bacterial topoisomerase I, a DNA topoisomerase I (topoI), is a novel target biomolecule for the discovery of new antibacterial drugs [1,2]. DNA topoisomerases play important roles on both the supercoiling control of DNA and the resolution of topological barriers during replication, transcription, and recombination [3–5]. The supercoiling tension caused by translocation of RNA polymerase must be relieved by topoisomerases [6,7]. Topoisomerase I cleaves and rejoins a single DNA strand during topoI-DNA reactions [8], which establishes a transient covalent linkage between these two macromolecules. These complexes can be trapped using topoisomerase inhibitors [2,8].

Topoisomerase I can catalyze interconversion of various topological isomers [9] and type IA topoisomerase catalytic activity requires Mg^{2+} [10]. In *Escherichia coli*, EctopoI removes excess negative supercoils in order to regulate DNA supercoiling [11]. EctopoI is a single polypeptide of 865 amino acids and tyrosine 319 is the active site tyrosine in EctopoI that forms a transient covalent linkage to DNA 5′ phosphoryl group during EctopoI-DNA reaction [12]. We quantitatively studied the interactions for EctopoI–pBAD/Thio supercoiled plasmid DNA (hereafter termed as pBAD/Thio) and Mg^{2+} bound EctopoI (Mg^{2+}EctopoI)–pBAD/Thio using the surface plasmon resonance (SPR) technique.

SPR is a widely used label free technique to determine equilibrium dissociation constants and the kinetics of bio-molecular interactions [13]. The sensor surface modification for the SPR assay was confirmed by using electrochemical impedance spectroscopy (EIS). The equilibrium dissociation constant (K_d) for EctopoI binding to pBAD/Thio was determined to be about 8 nM. A slightly higher K_d (~15 nM) value was obtained for Mg^{2+}EctopoI–pBAD/Thio interactions. In addition, the dissociation rate constants (k_d) for the interactions between the enzymes (EctopoI or Mg^{2+}EctopoI)

* Corresponding authors. Fax: +1 (305) 348 3772 (Y.-C. Tse-Dinh), +1 (305) 348 6700 (J. He, Y. Darici).
E-mail addresses: ytsedinh@fiu.edu (Y.-C. Tse-Dinh), jinhe@fiu.edu (J. He), dariciy@fiu.edu (Y. Darici).

http://dx.doi.org/10.1016/j.bbrc.2014.02.015
0006-291X/

and pBAD/Thio were also derived and a larger k_d was obtained for Mg^{2+}EctopoI–pBAD/Thio interactions. These results can help us further understand the important role of Mg^{2+} in the interactions between EctopoI and DNA substrate during catalysis [14].

Mycobacterial tuberculosis topoisomerase I (MttopoI), has a different C-terminal DNA binding domain (CTD) that lacks the three Zn^{2+} binding motifs in the CTD of EctopoI [15]. Binding to pBAD/Thio plasmid DNA by the two enzymes were compared. Under our experimental conditions, weak SPR signals were observed for interactions between MttopoI and pBAD/Thio. Therefore, the K_d value could not be recovered for MttopI–pBAD/Thio interactions.

2. Materials and methods

2.1. Materials

Triethylene glycol mono-11-mercaptoundecyl ether (PEG-thiol), nickel (II) sulfate hexahydrate, sodium, chloride, potassium hexacyanoferrate (III) and ethanolamine HCl were purchased from Sigma–Aldrich, ethanol (200 proof) from Decon Laboratories LLC, 2-{2-[2-(1-mercaptoundec-11-yloxy)-ethoxy]-ethoxy)-ethoxy nitrilotriacetic acid (NTA-thiol) from ProChimia Surfaces, Poland and potassium ferrocyanide trihydrate from Acros Organics. N-hydroxysuccinimide (NHS), N-(3-dimethylaminopropyl)-N′-ethyl-carbodiimide hydrochloride (EDC) and GeneJET Plasmid Maxiprep Kit were received from Thermo-Scientific. All other reagents were purchased from VWR international, Randor, PA, USA. Solutions were prepared using deionized (DI) water (~18 MΩ) (Ultra Purelab system, ELGA/Siemens or Milli-Q Direct 8 water system). The polycrystalline gold chips (50 nm Au over 2.5 nm titanium adhesion layers, coated on 18 mm × 18 mm cover slip glass slides) were purchased from Platypus Technologies, LLC, Madison, WI and each chip was cut into two halves before further processing.

2.2. Methods

2.2.1. Isolation and purification of EctopoI, MttopoI and pBAD/Thio

Recombinant EctopoI and MttopoI were expressed and purified as N-terminal His-tagged proteins according to previously reported procedures [16,17]. For the SPR experiments, the EctopoI was dialyzed against HEPES buffer (10 mM Hepes, pH 7.4 containing 100 mM NaCl and 0.005% (V/V) tween 20 in DI water) overnight at 4 °C. The MttopoI was dialyzed against HEPES buffer with 2.5% (V/V) glycerol overnight at 4 °C. The glycerol was needed to maintain solubility of MttopoI. The pBAD/Thio supercoiled plasmid DNA was purified using Genejet maxiprep kit (Thermo Scientific) according to the manufacturer's protocol.

2.2.2. Sensor preparation and characterization

Gold chips were used to prepare SPR sensors. After rinsing in ethanol for 2–3 min, the chips were cleaned by oxygen plasma (Plasma Cleaner PDC-001, Harric Plasma, Ithaca, NY) for 40 s at an oxygen pressure of 500–600 mTorr and RF power of 10.2 W. The chips were then annealed with hydrogen flame for 20 s to reduce the surface roughness [18]. To form a self-assembled monolayer (SAM), the hydrogen flamed chip was immediately immersed in mixed thiol solution (1:9 V/V mixture of 1 mM NTA-thiol and 1 mM PEG-thiol in ethanol respectively) and incubated overnight. The chip was then copiously rinsed with ethanol and DI water to remove physically adsorbed thiol molecules and dried with argon. The formation of SAM on the cleaned gold surface was confirmed by electrochemical impedance spectroscopy (EIS). A detailed explanation of EIS experiments can be found in Supplementary information (Section S1). Fig. 1A shows the scheme of SAM formation and His-tagged EctopoI or MttopoI immobilization. The modified chip was then mounted inside SPR flow cell. The detail of a similar SPR system can be found in a previous report [19].

2.2.3. Enzyme immobilization and DNA binding

The sensor surface was activated using a 40 mM nickel (II) sulfate solution prepared in DI water for 2 min at a flow rate of 50 μL/min followed by DI water flushing for 2 min. The surface was then equilibrated with the HEPES buffer for 5–10 min. His-tagged EctopoI (2 μM) or MttopoI (2.5 μM) was immobilized on the activated SAM surface at a flow rate of 50 μL/min via the capture covalent method [20]. Sequential treatment of the EctopoI or MttopoI immobilized surface was accomplished with a pulsed injection of NHS-EDC solution (25 mM NHS and 100 mM EDC) in DI water followed by 1 M ethanolamine (pH 8.2) in DI water. This treatment allowed us to achieve the capture covalent immobilization. The experiments with various pBAD/Thio concentrations were accomplished by regeneration of the sensor surface using 1 M NaCl. For the experiments involving Mg^{2+}, 0.5 mM $MgCl_2$ (in Tris buffer, pH 8.0) was passed over EctopoI immobilized surface for 5 min. All the experiments were carried out at 22 °C.

2.2.4. Data analysis

Complex non-linear least square (CNLS) fitting algorithm was used for EIS data using an equivalent circuit model (Supplementary information, Section S1). Equilibrium data analysis methods were used to analyze the SPR data [21]. The simple nonlinear hyperbolic (SNLH) equation (Eq. (1) below) was used to fit the equilibrium SPR response plotted vs DNA concentrations,

$$R = \frac{R_{max}[DNA]}{K_d + [DNA]} \quad (1)$$

where, R is the equilibrium response, [DNA] is the analyte (pBAD/Thio) concentration, K_d is the equilibrium dissociation constant, and R_{max} is the fitting parameter representing the response at very high pBAD/Thio concentration. The dissociation rate constants were

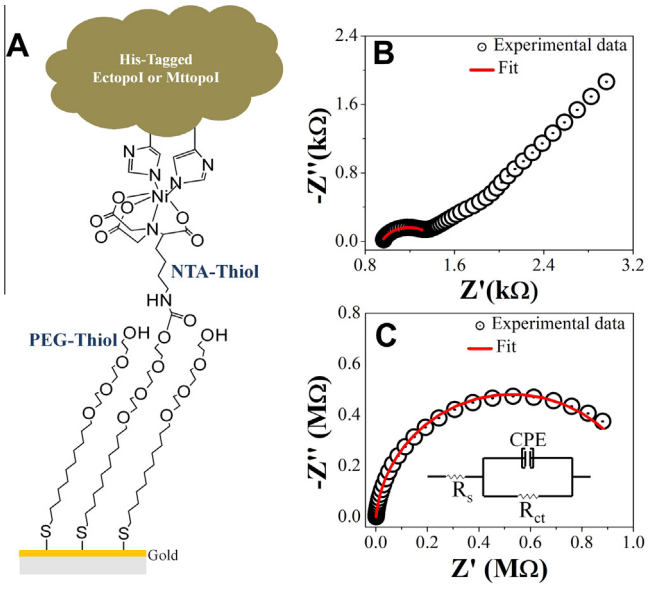

Fig. 1. (A) Scheme showing the sensor surface modification with mixed thiols followed by the His-tagged EctopoI or MttopoI immobilization. (B) electrochemical impedance spectroscopy (EIS) for the bare gold. (C) EIS for SAM modified gold surface, inset: equivalent circuit for EIS data fitting and analysis. CPE is the constant phase element, R_s is the solution resistance and R_{ct} is the charge transfer resistance. A frequency range from 10^{-1} Hz to 10^4 Hz was used during EIS measurements. In both figures B and C, the symbols are experimental data and continuous lines are the CNLS fit (see Supplementary information, Section S1, for details).

Table 1
The parameters obtained by CNLS fitting of EIS experimental data to an equivalent circuit (Inset, Fig. 2C). The errors are the standard errors of the fitting.

Surface	C (nF)	R_{ct} (kΩ)	R_s (kΩ)	α
Au	1227 ± 122	0.48 ± 0.08	0.95 ± 0.04	0.75 ± 0.01
Au/SAM	313 ± 3	1060 ± 10	0.93 ± 0.08	0.94

also derived by fitting the SPR dissociation profiles. A detailed explanation of the fitting procedure is given in the Supplementary information (Section S2).

3. Results

3.1. Sensor surface characterization

As shown in Fig. 1B and C, the EIS experimental data (symbols) are fitted (continuous lines) using the equivalent circuit (inset, Fig. 1C). The parameters obtained from fitting are listed in Table 1. The charge transfer resistance (R_{ct}) for SAM modified gold is significantly higher (~1060 kΩ) compared to cleaned bare gold (~0.5 kΩ). This clearly confirms the successful modification of the gold surface. Furthermore, due to the presence of SAM on the gold surface, the interfacial capacitance (C) for modified surface is obviously reduced (313 nF) compared to clean gold (1227 nF).

3.2. Enzyme immobilization and pBAD/Thio binding

As explained in the methods section, both EctopoI (Fig. 2A) and MttopoI (Fig. S3, Supplementary information) were immobilized onto the Ni^{2+} chelated NTA surface via the capture covalent method. Fig. 2B depicts the sensor surface stability after chemical treatment of the enzyme immobilized surfaces with NHS-EDC followed by ethanolamine. Fig. 2C is the representation of pBAD/Thio binding to the enzyme immobilized sensor surfaces, including association, saturation and dissociation of SPR signal. The sensor surface was regenerated using 1 M NaCl solution.

3.3. pBAD/Thio molecular interaction with EctopoI, Mg^{2+}EctopoI and MttopoI

The concentration-dependent pBAD/Thio binding to EctopoI and Mg^{2+}EctopoI are shown in Fig. 3A and B, respectively. Under our experimental conditions, the pBAD/Thio did not show a considerable response change upon its binding to MttopoI (Fig. 3C). The SNLH fitting, using Eq. (1), to the plot of equilibrium response vs. concentration of pBAD/Thio (Fig. 3D) provides quantitative information of the interaction; more precisely, the K_d can be derived. The K_d value obtained from the fit is about 8 nM for EctopoI–pBAD/Thio interactions and a slightly higher K_d value (~15 nM) for Mg^{2+}EctopoI–pBAD/Thio interactions. We could not obtain quantitative information for MttopoI–pBAD/Thio interactions.

3.4. Effect of Mg^{2+}on EctopoI–pBAD/Thio molecular interaction

To study the effect of Mg^{2+}, the SPR dissociation signals were fitted using the exponential dissociation rate constant equation (Supplementary information, Section S2). As shown in Fig. 4, stronger dissociation signals were observed for Mg^{2+}EctopoI–pBAD/Thio interactions compared to EctopoI–pBAD/Thio interactions. The derived dissociation rate constant (k_d) value for EctopoI–pBAD/Thio interactions is ~0.017 s^{-1} and for Mg^{2+}EctopoI–pBAD/Thio interactions is ~0.043 s^{-1}. Compared to EctopoI–pBAD/Thio interactions, a larger k_d value for Mg^{2+}EctopoI–pBAD/Thio interactions suggests that the rate of enzyme turnover following DNA religation during catalysis of EctopoI–pBAD/Thio relaxation reaction is enhanced in the presence of Mg^{2+}.

4. Discussion

Recognizing EctopoI as an important target biomolecule for the discovery of new antibacterial drugs [1], EctopoI–plasmid DNA interactions were quantitatively studied for the first time (to the best of our knowledge) using SPR, a surface based affinity technique. In the SPR technique, the sensor surface modification plays a crucial role for the minimization of non-specific binding and reproducibility of SPR signals. We carried out EIS measurements to confirm the gold surface modification via the mixed thiols (Supplementary information, Section S1). The efficient charge (electron) transfer between the redox couple and the working electrode in solution is basically evaluated by charge transfer resistance (R_{ct}) determination. The R_{ct}, obtained either from fitting or crudely from the semicircular diameter (Fig. 1B and C) [22], for Au surface is much smaller compared to Au/SAM surface (Table 1). This clearly confirms the successful sensor surface modification.

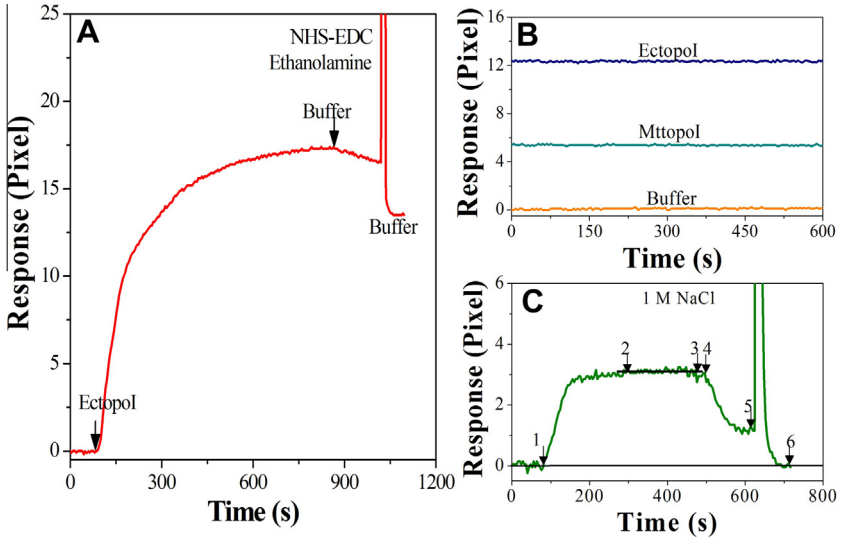

Fig. 2. (A) SPR sensorgram for the immobilization of EctopoI via capture covalent method. The arrows show the start of immobilization and buffer wash. (B) Representative SPR signals showing stability of sensor surface; with buffer before enzyme immobilization and after capture covalent immobilization of the enzymes. (C) Representative SPR profile for EctopoI–pBAD/Thio interaction: 1–2 association, 2–3 saturation, 3–4 minor signal shift due to manual changing of valve, 4–5 dissociation, and 5–6 regeneration.

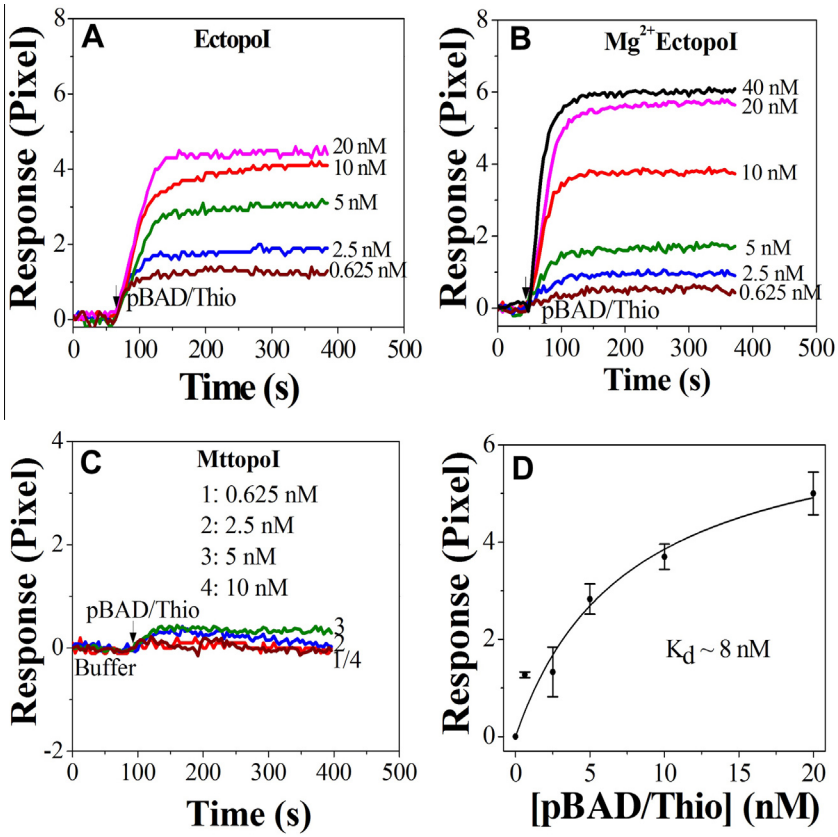

Fig. 3. SPR sensorgrams for (A) pBAD/Thio binding to EctopoI, (B) for pBAD/Thio binding to Mg^{2+} bound EctopoI and (C) for pBAD/Thio binding to MttopoI. (D) Plot of equilibrium SPR response vs pBAD/Thio concentration. The symbols are average experimental data of three different measurements with error bars as standard deviation and the continuous lines are the simple hyperbolic fit (explained in text).

Our data also show that the interfacial capacitance (C) decreases as the surface thickness increases because of the surface modification (Table 1). The successful immobilization of EctopoI or MttopoI on the modified sensor surface was achieved via capture covalent method. Previously reported result shows that the single histidine tag has a weak affinity (~1 μM) to the Ni^{2+}-NTA surface [23]. Even immobilized hexahistidine tagged proteins would dissociate upon continuous buffer flushing, and this phenomenon is not suitable for protein-small molecule interaction studies [20]. The immobilized enzyme surface must therefore be stable. This can be achieved by chemical treatment of the enzyme immobilized surface with sequential flow of NHS-EDC and ethanolamine solutions [20] (explained in methods). 30 μL of each solution was injected as a pulse for 20 s. Figs. 2A and S3 (Supplementary information) show the EctopoI and MttopoI immobilization, respectively, onto the sensor surface via capture covalent immobilization. As shown in Fig. 2B, the SPR response was found to be stable for 10 min before and after the treatment of EctopoI and MttopoI immobilized surfaces and thus guarantees the sensor surface stability and the successful capture covalent immobilization of the enzymes.

Fig. 3A shows the interaction of EctopoI–pBAD/Thio in a concentration dependent manner. The EctopoI–pBAD/Thio binding responses saturated quickly; therefore an equilibrium analysis method could easily produce the K_d value via SNLH fitting (Fig. 3D). The K_d value for EctopoI–pBAD/Thio interactions was found to be about 8 nM. A slightly higher K_d value (~15 nM) was obtained for Mg^{2+}EctopoI–pBAD/Thio interactions. For the experiments shown in Fig. 3A and B, except for 40 nM data, each SPR trace was repeated three times. Due to sample limitation, the 40 nM data was not repeated. After saturated SPR responses were achieved, dissociation SPR profiles were recorded for some experiments. Buffer flushing could dissociate the EctopoI–pBAD/Thio complex considerably. The covalent topoisomerase–DNA complex is transient and reversible in nature [4]. Treatment of the topoisomerase–DNA complex with high salt would promote dissociation of the DNA from enzyme following religation [24]. After desired SPR signals were recorded, the surface was treated using 1 M NaCl (in DI water) via pulsed injection for 2–3 min. This could successfully regenerate the surface to the initial (buffer) level and the surface was ready for next pBAD/Thio concentration. Fig. 2C shows a typical SPR sensorgram showing association, saturation and dissociation of enzyme–pBAD/Thio interaction followed by regeneration. It should be noted that 10 mM Tris (pH 8.0) buffer was used as running buffer for enzymes–pBAD/Thio interaction experiments. The immobilized enzyme surfaces were equilibrated with the Tris buffer, for approximately 5 min, before pBAD/Thio injection. The experiments for each enzyme were performed either on the same chip or on different sensor chips. The variation of chip surfaces resulted in a variation of equilibrium response (lowest to highest) of ~0.6 pixels, on an average.

In order to understand the influence of the topoI C-terminal CTD sequence on the interactions between topoI and supercoiled plasmid DNA, we also studied the interaction between MttopoI and pBAD/Thio using SPR. There are tetracysteine Zn^{2+} binding motifs [25] that follow the N-terminal 67 kDa transesterification domain [26]. The three tetracysteine motifs are part of a DNA-binding domain at the C-terminus of EctopoI [27]. Unlike EctopoI [28], MttopoI lacks Zn^{2+} coordination and has evolved to have a different CTD sequence [15]. Under our experimental conditions, we could not see the concentration dependent interaction for MttopoI–pBAD/Thio interactions. As shown in Fig. 3C, weak SPR signals were observed instead. This result suggests that the tetracysteine Zn^{2+} binding motifs

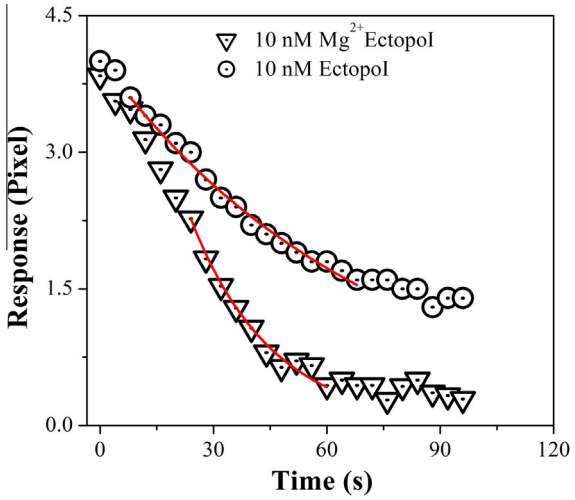

Fig. 4. Representative SPR dissociation profiles fitted to exponential dissociation rate equation (Eq. S2a, Supplementary information). The symbols are experimental data and the continuous lines are the best fit to the rate equation, S2a.

are required for observing the interaction with plasmid DNA with the SPR protocol described here. *Mycobacterium smegmatis* topoisomerase I (Mstopol) has a CTD similar to MttopoI that also does not coordinate Zn^{2+} [15]. Previous reports indicate that MstopoI CTD interacts with DNA during catalysis [29] and is responsible for sequence specific recognition of duplex DNA by Mstopol [30]. Because of its specific interaction with duplex DNA sequence, the *Mycobacterium topoisomerase* CTD may not be as efficient in promoting high affinity binding to the single-stranded DNA region in supercoiled plasmid DNA as the CTD in EctopoI. Alternatively, the result observed here might be due to the loss of MttopoI activity during protein immobilization. The dialyzed MttopoI sample used for protein immobilization was assayed for relaxation activity and found to be active (Fig. S4, Supplementary information).

It has been revealed from the crystal structure of the 67 kDa N-terminal fragment of EctopoI that there is presence of acidic and basic amino acid residues nearby the active site region [31]. It has also been proposed that Lys-13 and Arg-321 (both basic residues) participate in DNA cleavage [32,33] and three acidic residues Asp-111, ASP-113, and Glu-115 coordinate with Mg^{2+} [34]. We could not detect the concentration dependent Mg^{2+} binding to EctopoI, which might be the limiting case of our SPR systems to resolve the detection of very small molecular weight ions/molecules–protein interactions. We also did not analyze our SPR sensorgrams for association rate constant measurements due to rapid association and fast saturation of the SPR signals. Therefore, to better understand the effect of Mg^{2+} coordination, the SPR dissociation profiles were recorded for the SPR sensorgrams shown in Fig. 3A and B. These SPR profiles were fitted to the exponential dissociation rate constant equation. The fitting procedure is explained in detail in the Supplementary information (Section S2). A larger dissociation rate constant (k_d) ($\sim$0.043 s^{-1}) was obtained for Mg^{2+}EctopoI–pBAD/Thio compared to EctopoI–pBAD/Thio interactions ($\sim$0.017 s^{-1}). This increase in k_d value confirms that EctopoI catalytic activity is enhanced with Mg^{2+}. This is consistent with the role of Mg^{2+} to increase the dissociation rate constants for type IB topoisomerase I–DNA interactions, as reported previously [14]. Such analysis for type IA topoisomerase–DNA interactions has not been previously reported.

Acknowledgments

P. Tiwari would like to thank Florida International University (FIU) School of Integrated Science & Humanity, College Arts & Sciences for the research assistantship. This work was supported by NIH Grant R01GM054226 (Y.T.) and the start-up funds from FIU (J.H.).

Appendix A. Supplementary data

Supplementary data associated with this article can be found, in the online version, at http://dx.doi.org/10.1016/j.bbrc.2014.02.015.

References

[1] Y.C. Tse-Dinh, Bacterial topoisomerase I as a target for discovery of antibacterial compounds, Nucleic Acids Res. 37 (2009) 731–737.
[2] B. Cheng, S. Shukla, S. Vasunilashorn, S. Mukhopadhyay, Y.C. Tse-Dinh, Bacterial cell killing mediated by topoisomerase I DNA cleavage activity, J. Biol. Chem. 280 (2005) 38489–38495.
[3] J.J. Champoux, DNA topoisomerases: structure, function, and mechanism, Annu. Rev. Biochem. 70 (2001) 369–413.
[4] J.C. Wang, Cellular roles of DNA topoisomerases: a molecular perspective, Nat. Rev. Mol. Cell Biol. 3 (2002) 430–440.
[5] K.D. Corbett, J.M. Berger, Structure, molecular mechanisms, and evolutionary relationships in DNA topoisomerases, Annu. Rev. Biophys. Biomol. Struct. 33 (2004) 95–118.
[6] L.F. Liu, J.C. Wang, Supercoiling of the DNA template during transcription, Proc. Natl. Acad. Sci. U.S.A. 84 (1987) 7024–7027.
[7] H.Y. Wu, S. Shyy, J.C. Wang, L.F. Liu, Transcription generates positively and negatively supercoiled domains in the template, Cell 53 (1988) 433–440.
[8] H.P. Tsai, L.W. Lin, Z.Y. Lai, J.Y. Wu, C.E. Chen, J. Hwang, C.S. Chen, C.M. Lin, Immobilizing topoisomerase I on a surface plasmon resonance biosensor chip to screen for inhibitors, J. Biomed. Sci. 17 (2010) 49.
[9] J.C. Wang, DNA topoisomerases, Annu. Rev. Biochem. 54 (1985) 665–697.
[10] C. Sissi, M. Palumbo, Effects of magnesium and related divalent metal ions in topoisomerase structure and function, Nucleic Acids Res. 37 (2009) 702–711.
[11] K. Drlica, Bacterial topoisomerases and the control of DNA supercoiling, Trends Genet. 6 (1990) 433–437.
[12] R.M. Lynn, J.C. Wang, Peptide sequencing and site-directed mutagenesis identify tyrosine-319 as the active site tyrosine of *Escherichia coli* DNA topoisomerase I, Proteins: Struct. Funct. Genet. 6 (1989) 231–239.
[13] W.D. Wilson, Analyzing biomolecular interactions, Science 295 (2002) 2103–2105.
[14] C.D. Pond, J.A. Holden, P.C. Schnabel, L.R. Barrows, Surface plasmon resonance analysis of topoisomerase I-DNA binding: effect of Mg^{2+} and DNA sequence, Anti-Cancer Drugs 8 (1997) 336–344.
[15] T. Bhaduri, T.K. Bagui, D. Sikder, V. Nagaraja, DNA topoisomerase I from *Mycobacterium smegmatis*: an enzyme with distinct features, J. Biol. Chem. 273 (1998) 13925–13932.
[16] E.P. Sorokin, B. Cheng, S. Rathi, S.J. Aedo, M.V. Abrenica, Y.C. Tse-Dinh, Inhibition of Mg^{2+} binding and DNA religation by bacterial topoisomerase I via introduction of an additional positive charge into the active site region, Nucleic Acids Res. 36 (2008) 4788–4796.
[17] T. Annamalai, N. Dani, B. Cheng, Y.C. Tse-Dinh, Analysis of DNA relaxation and cleavage activities of recombinant *Mycobacterium tuberculosis* DNA topoisomerase I from a new expression and purification protocol, BMC Biochem. 10 (2009) 18.
[18] M.C. Leopold, E.F. Bowden, Influence of gold substrate topography on the voltammetry of cytochrome c adsorbed on carboxylic acid terminated self-assembled monolayers, Langmuir 18 (2002) 2239–2245.
[19] N.M. Mulchan, M. Rodriguez, K. O'Shea, Y. Darici, Application of a high-resolution SPR technique for monitoring real-time metal/dielectric interactions, Sens. Actuators, B 88 (2003) 132–137.
[20] M.A. Wear, A. Patterson, K. Malone, C. Dunsmore, N.J. Turner, M.D. Walkinshaw, A surface plasmon resonance-based assay for small molecule inhibitors of human cyclophilin A, Anal. Biochem. 345 (2005) 214–226.
[21] A.E.M. Wammes, M.J.E. Fischer, N.J. de Mol, M.B. van Eldijk, F.P.J.T. Rutjes, J.C.M. van Hest, F.L. van Delft, Site-specific peptide and protein immobilization on surface plasmon resonance chips via strain-promoted cycloaddition, Lab Chip 13 (2013) 1863–1867.
[22] Y.P. Shan, P.B. Tiwari, P. Krishnakumar, I. Vlassiouk, W.Z. Li, X.W. Wang, Y. Darici, S.M. Lindsay, H.D. Wang, S. Smirnov, J. He, Surface modification of graphene nanopores for protein translocation, Nanotechnology 24 (2013) 495102.
[23] L. Nieba, S.E. Nieba-Axmann, A. Persson, M. Hämäläinen, F. Edebratt, A. Hansson, J. Lidholm, K. Magnusson, Å.F. Karlsson, A. Plückthun, BIACORE analysis of histidine-tagged proteins using a chelating NTA sensor chip, Anal. Biochem. 252 (1997) 217–228.
[24] S.J. Chen, J.C. Wang, Identification of active site residues in *Escherichia coli* DNA topoisomerase I, J. Biol. Chem. 273 (1998) 6050–6056.
[25] Y.C. Tse-Dinh, R.K. Beran-Steed, *Escherichia coli* DNA topoisomerase I is a zinc metalloprotein with three repeatitive zinc-binding domains, J. Biol. Chem. 263 (1998) 15857–15859.
[26] A. Ahumada, Y.C. Tse-Dinh, The role of the Zn(II) binding domain in the mechanism of *E. coli* DNA topoisomerase I, BMC Biochem. 3 (2002) 13.

[27] A. Ahumada, Y.C. Tse-Dinh, The Zn(II) binding motifs of *E. coli* DNA topoisomerase I is part of a high-affinity DNA binding domain, Biochem. Biophys. Res. Commun. 251 (1998) 509–514.
[28] L. Yu, C.X. Zhu, Y.C. Tse-Dinh, S.W. Fesik, Solution structure of the C-terminal single-stranded DNA-binding domain of *Escherichia coli* topoisomerase I, Biochemistry 34 (1995) 7622–7628.
[29] W. Ahmed, A.G. Bhat, M.N. Leelaram, S. Menon, V. Nagaraja, Carboxyl terminal domain basic amino acids of mycobacterial topoisomerase I bind DNA to promote strand passage, Nucleic Acids Res. 41 (2013) 7462–7471.
[30] T. Bhaduri, D. Sikder, V. Nagaraja, Sequence specific interaction of *Mycobacterium smegmatis* topoisomerase I with duplex DNA, Nucleic Acids Res. 26 (1998) 1668–1674.
[31] C.D. Lima, J.C. Wang, A. Mondragon, Three-dimensional structure of the 67K N-terminal fragment of *E. coli* DNA topoisomerase I, Nature 367 (1994) 138–146.
[32] D. Strahs, C.X. Zhu, B. Cheng, J. Chen, Y.C. Tse-Dinh, Experimental and computational investigations of Ser10 and Lys13 in the binding and cleavage of DNA substrates by *Escherichia coli* DNA topoisomerase I, Nucleic Acids Res. 34 (2006) 1785–1797.
[33] H. Feinberg, C.D. Lima, A. Mondragón, Conformational changes in *E. coli* DNA topoisomerase I, Nat. Struct. Biol. 6 (1999) 918–922.
[34] C.X. Zhu, Y.C. Tse-Dinh, The acidic triad conserved in type IA DNA topoisomerases is required for binding of Mg(II) and subsequent conformational change, J. Biol. Chem. 275 (2000) 5318–5322.